EXPERIMENTAL INVESTIGATION OF ITG-LIKE TURBULENCE CHARACTERISTICS IN T-10 TOKAMAK CORE PLASMA WITH TOROIDAL AND POLOIDAL CORRELATION REFLECTOMETRY

VERSHKOV V.A., SOLDATOV S.V., SHELUKHIN D.A., CHISTIAKOV V.V.
Russian Research Center «Kurchatov Institute» 123182 Moscow, Russia.

Abstract

The physical mechanisms of small-scale density fluctuations in the frequency range 5 - 500 kHz have been investigated with correlation reflectometry in different types of ohmicaly heated discharges. A temporal formation of velocity shear in the central region of plasma column during the discharge transition from Saturated to Improved Ohmic Confinement results in suppression of long wavelength quasi-coherent turbulence, while the amplitude of fluctuations with shorter wavelength is not affected. The potential of correlation reflectometry was extended by simultaneous plasma probing from Low Field Side and High Field Side. A factor of 5 enhancement of quasi-coherent turbulence at Low Field Side was measured, while the other turbulence type is poloidally symmetrical. Nearly 100 % long distance toroidal correlation was observed for quasi-coherent density fluctuations at a distance of 10 meter after one turn around tokamak major axis. Fluctuations propagate at an angle of about 0.5^{0} with respect to the perpendicular to the magnetic field line, proving a drift mechanism of turbulence. A plasma rotation was estimated from the radial force balance equation for ions with the radial electric field, measured with heavy ion beam probe diagnostic. A comparison of the calculated plasma rotation with measured turbulence one show that the turbulence either rotates in ion diamagnetic drift direction in a plasma frame. All experimental observations are consistent with Toroidal and Slab ITG turbulence physical mechanism.

1. INTRODUCTION

A spectacular progress in investigations of the anomalous turbulent transport in tokamaks have been made during last years. For the first time it was established unambiguously direct relation between plasma anomalous transport and amplitude of small scale turbulence [1]. It was shown that a velocity shear is able to reduce a turbulence amplitude or even to suppress it at all. The turbulence suppression can be described theoretically [2] with the combination of Ion Temperature Gradient ITG [3] and Trapped Electron Mode TEM [4] instabilities. It was found in TFTR experiments with Beam Emission Spectroscopy (BES) [5] that core turbulence is «unimodal» and rotates in ion diamagnetic drift direction in a plasma frame. Nevertheless the investigation of small-scale turbulence structure, its physical mechanism and comparison with theoretical predictions under different discharge conditions are still important topics of tokamak experiment. They were the main motivation of T-10 turbulence investigations [6-10], new results are presented in this paper.

The behavior of core density fluctuations have been investigated during the discharge transition from Saturated to Improved Ohmic Confinement (SOC to IOC) [11]. The potential of correlation reflectometry was significantly enhanced by means of simultaneous plasma probing from Low Field Side (LFS) and High Field Side (HFS) which gave the opportunity to observe a poloidal asymmetry and long distance toroidal correlations of density fluctuations. The turbulence rotation in a plasma frame was obtained by the comparison of measured turbulence velocity with the plasma rotation calculated from an ion radial force balance equation. The experimental data are compared with theoretical predictions for Toroidal [12] and Slab [3] ITG turbulence.

2. EXPERIMENTAL SETUP

Density fluctuations in frequency range 5 - 500 kHz have been investigated with the T-10 heterodyne correlation reflectometry [13] mainly in ohmicaly heated discharges. The reflection of O-mode was used in the frequency range 36—78 GHz. The upgraded antenna system is located on the top port of tokamak and consisted of two antenna arrays aligned to the center of the plasma column. The first one is set at an angle of 29^{o} with vertical direction towards LFS. The second one is set at an angle of 26^{o} with vertical direction towards HFS. It was possible to probe the plasma simultaneously

from both the HFS and the LFS in order to measure the poloidal asymmetry of the turbulence. The special precautions were taken to reduce possible parasitic coherency between the different reflected signals. The frequency fluctuations of a reference Intermediate Frequency (IF) was recorded together with the amplitude fluctuations of reflected waves. The experimentally observed low level of parasitic coherency between the amplitude fluctuations of different reflected waves gave opportunity to reduce the lowest significant value of coherency to a few percent. A slow phase variation of the reflected wave was also recorded to monitor the relative variation of a distance to cutoff layer.

3. TURBULENCE BEHAVIOR DURING DISCHARGE TRANSITION FROM SOC TO IOC MODE.

The core turbulence behavior of high density plasma during transition from SOC to IOC [11] regime after gas puff cutoff [14] was observed for the first time by means of O-mode correlation reflectometry with a frequency band from 53 to 78 GHz. The plasma current I_p was 200 kA, toroidal magnetic field B_T =2.5 T and density $n_e=4.2\times10^{19}$ m^{-3}.A process of strong density peaking after gas cutoff have a form of the wave of strong gradient travelling from periphery to the center with characteristic time 150 ms. The turbulence behavior during the transition at three radial positions of reflected layer are shown in Fig. 1. The level of «broad band» turbulence steadily decreases after gas cutoff while level of «quasi-coherent» fluctuations starts to increase in accordance with previous observation at the edge [9]. The amplitude of «broad band» reaches the minimum and then rises again. The time delay of the minimum with respect to gas puff cutoff increases as the reflection radius decreases as shown by the oblique dashed line in Fig. 1 b-d. The process looks like a wave of turbulence suppression traveling from plasma periphery to the center. The turbulence suppression may be explained by experimentally observed velocity shear of turbulence which is shown in Fig. 2. The turbulence velocities were obtained by means of time delay measurements between fluctuations observed at two poloidally separated points. The incident wave is launched from the middle horn of LFS antenna array and is received by the two side antennas. A time delay of the velocity increase in the center can be seen in Fig. 2 which implies the existence of the temporal velocity shear region between outer and inner discharge layers. The computer simulation of density profile evolution showed the necessity to use the transport barrier in calculations. New phenomenon of «quasi-coherent» fluctuations suppression in a core plasma is clearly seen in Fig. 1c at τ_3=465 ms. A time evolution of the amplitude and poloidal coherency spectra for the signal in Fig. 1c are shown at the bottom for the four times indicated by the arrows. One can see that the amplitude and coherency maximums of the «quasi-coherent» fluctuations at 120 kHz are present at τ_2 and τ_4 but are absent at τ_2. At the same time the fluctuations with the frequency of 220 kHz are not affected. The residual new type of «quasi-coherent» fluctuations at 220 kHz have $\lambda_\perp$=0.9 cm and $k_\perp\times\rho_i$=1. This mode is present before and also later together with usual «quasi-coherent» fluctuations with frequency 120 kHz, $\lambda_\perp$=1.8 cm and $k_\perp\times\rho_i$=0.5. Thus one can see that velocity shear value may be enough to suppress a longer wavelength turbulence but can't stabilize shorter waves. This fact shows the presence of two different turbulence types. Despite of the fact that turbulence amplitude practically returns to the initial value before the gas cutoff the simulations of density behavior show more then a factor of three reduction of a diffusion coefficient. This let us to suppose that a plasma transport is not determined only by the amplitude but also by the phase relation between the density and radial velocity fluctuations.

4. POLOIDAL ASYMMETRY MEASUREMENTS

Poloidal asymmetry measurements can be realized by comparison of reflected-wave phase fluctuations received by the LFS and HFS antennas. Such comparison of the amplitude spectra of frequency fluctuations is shown in Fig. 3 for two ohmic T-10 discharges. In the case of Fig. 3a the LFS amplitude is higher and differs qualitatively from the HFS spectrum. In particular, two maxima are clearly seen in the spectrum of the LFS signal which are several times lower in the HFS spectrum.

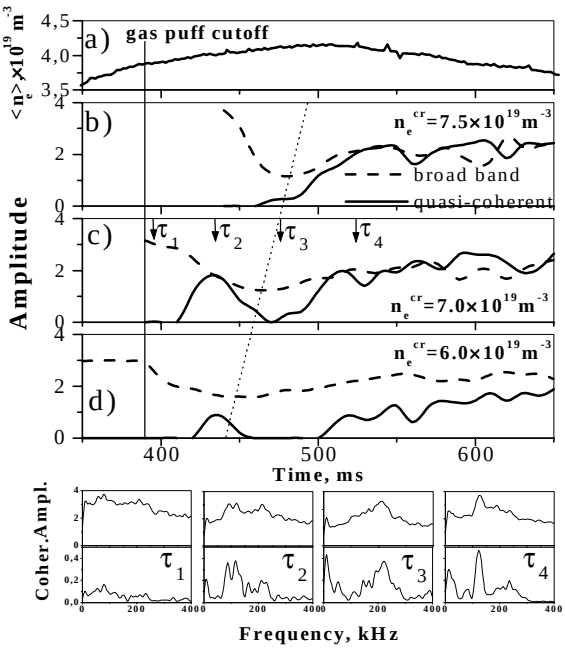

FIG. 1.

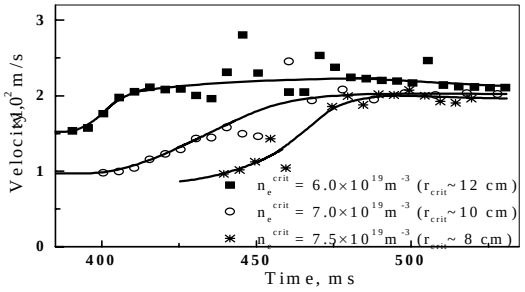

Fig2

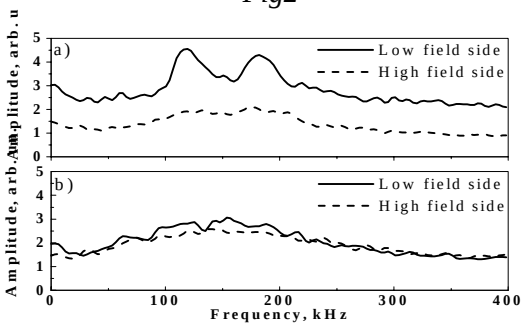

FIG. 3.

FIG. 1. Time evolution of turbulence amplitudes at three radial cutoff positions during SOC to IOC transition. a) average density; b), c), d) amplitudes of «broad band»-dashed line and «quasi-coherent»-solid line for three reflection cutoff positions. At the bottom-the amplitude and coherency spectra for the four times, marked in Fig. 1c.
FIG. 2 The fluctuations velocities at three reflection radius during SOC to IOC transition. (squares- r~12 cm; circles- r~10 cm; stars- r~ 8 cm).
FIG. 3. The amplitude Fourier spectra of the turbulence at LFS - solid line and HFS - dashed line for two discharge conditions. a) - case of high asymmetry; b) - symmetrical case.

In contrast, both spectra practically coincide in the discharge shown in Fig. 3b.A variety of asymmetry measurements gives ground to conclude that two different types of the turbulence may be responsible for observed difference in the poloidal asymmetry. The first turbulence type is present in spectrum as two narrow maxima in Fig 3a and has been previously observed at the LFS as «quasi-coherent» bursts of monochromatic oscillations [7]. It is highly asymmetrical poloidally and usually has two peaks in the amplitude Fourier spectrum. The second type can be seen in Fig 3b which have a smooth maximum at 160 kHz and is poloidally symmetrical. It is obvious that both spectra in Fig 3a may be explained as a mixture of both kinds of turbulence. The experimental data also let us to conclude that a «broad band» increase at the LFS in Fig 3a is in some way associated with the appearance of «quasi-coherent» bursts. This may be either due to an intrinsic nonlinear transformation of energy in the turbulence spectrum or due to a specific reflectometry broadening of the spectrum. One of the possible explanation is the simultaneously existence of symmetrical so called «slab» ITG [3] driven by the gradients of temperature and density and highly asymmetrical «toroidal» ITG driven by the curvature effects [12]. Additional insight into relation of both turbulence types may give the variation of turbulence amplitude at LFS and HFS during sawtooth crashes and ECR heating. It was found that high poloidal turbulence asymmetry before the crash usually becomes symmetrical after the crash. It may be connected with the increase of gradients after the crash which is the driving term of symmetrical Slab ITG turbulence. The turbulence amplitude also becomes symmetrical in ECR heated discharges.

5. LONG DISTANCE TOROIDAL CORRELATION MEASUREMENTS

Due to the fact that the magnetic field in tokamak is the sum of toroidal and poloidal fields the lines of total magnetic field are helical. The helical field line coiling round the torus forms the magnetic surface. In tokamak the surfaces of equal density coincide with the magnetic ones. As our reflectometer operates in the ordinary mode the reflection points at any poloidal launch angles automatically remain at the same magnetic surface. The helical transform is characterized by the safety factor q,

$$q=(B_{tor}\bullet r)/(B_{pol}\bullet R)$$

where B_{tor} and B_{pol} are the toroidal and poloidal magnetic fields, respectively, and r and R are minor and major tokamak radii. The poloidal angle after one turn of magnetic field line around tokamak major axis equals 360°/q. As the plasma freely moves along the field lines the density perturbations may be correlated at long distance. So the mapping of magnetic field lines is possible with several antennas placed at different poloidal and toroidal locations by means of the correlation technique. Such long distance toroidal correlations were proposed for the measurement of the q value [15]. In the case of T-10 the reflection spots of LFS and HFS side antennas can be connected along the magnetic field line at a safety factor q=0.87 or 1.16 after one turn around axis of the torus, and at q=1.74 or 2.32 after two turns. Two values of resonant q can be understood by the fact that from each antenna there are always two ways to reach the other antenna: clockwise and counterclockwise. An example of such long distance toroidal correlations between frequency fluctuations of the waves reflected from LFS and HFS is shown in Fig. 4. Figures 4a-c present amplitude spectra, cross-phase and coherency between LFS and HFS channels respectively. There is an obvious maximum in the coherency spectrum at frequency120 kHz. The slope of the cross-phase at this frequency corresponds to the time delay of 13 μs. The frequency of the maximum exactly coincides with the maximum in the amplitude spectrum of the LFS antenna. Figures 4d-f present cross-correlation functions for both channels which were taken for three close probing radii and filtered in the frequency range 100 - 140 kHz where quasi-coherent fluctuations are observed. About 30 cross-correlation functions with a time realization of 256 μs were averaged to decreased the noise level. It is clearly seen that the highest correlation value 0.4 corresponds to a zero time delay, which occurred at the minimal radius. As the reflection radius increases slightly due to a density rise the maximal value of cross-correlation decreases and time delay of its maximum increases. The curves of Fig 4e corresponds to the curve of Fig 4b. It can be seen that the time delay determined from the slope of the cross-phase and the shift of the maximum of the cross-correlation function both give the same value. As seen from Fig. 4a both coherent and incoherent fluctuations are present in the frequency range 100-140 kHz and the resulting value of cross-correlation is determined not only by the correlation properties of a quasi-coherent oscillations themselves but also by their relative representation in spectra of both signals. Nevertheless the main physical issue is the value of toroidal correlation for the coherent component alone. A computer simulation to decompose both signals to coherent and incoherent components was performed. It was supposed in simulations that cross-correlation of coherent component is equal to 1 and its representation in both signals were taken as in the experiment. It was found that under this conditions the value of maximum of cross-correlation function equals to 0.4. Thus one can conclude that the experimental value 0.4 is consistent with cross-correlation near 1 for quasi-coherent turbulence .The sign of the time delay proves unambiguously that this resonance correspond to q=0.87 although it is observed near the q=1 surface as it follows from the behavior of the phase of the reflected wave between sawtooth crashes. Thus it is possible to conclude that this wave propagates at an angle of about 0.5^0 with respect to a direction perpendicular to the total magnetic field as it is expected for drift waves. This is indication of a drift origin of these waves.

A special investigation of the long distance toroidal correlations was carried out. The plasma current was 200 kA and B_T=2.36 T. The reflection layer was varied by a slow 15 % density ramp down in a stationary phase of a series of successive discharges in the range of average densities from 1.5 to 2.5×10^{19} m^{-3}. Three probing frequencies 56, 48 and 40.8 were used to cover the range of

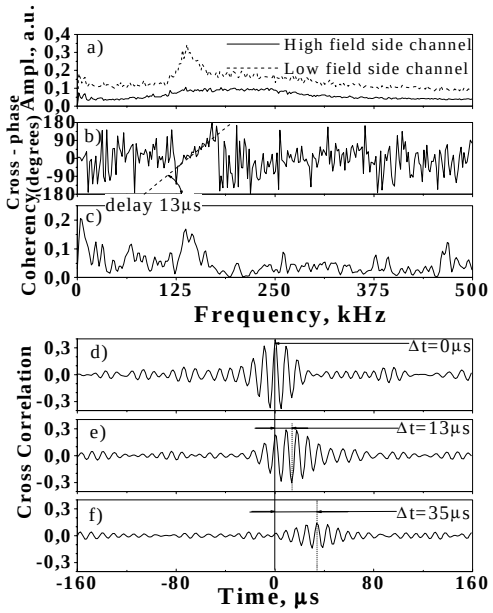

FIG. 4

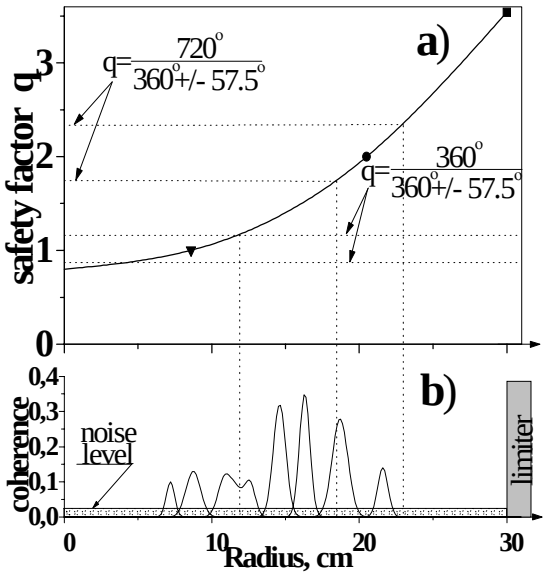

FIG. 5

FIG. 4. Long distance toroidal correlations between LFS and HFS antennas. a) - amplitude Fourier spectra of two frequency discriminators, solid line - HFS, dashed line - LFS; b)-cross-phase spectrum; c)- coherency spectrum; d) - f) -three cross-correlation functions for successively increasing reflected radii.

Fig. 5. Radial locations of the long distance toroidal correlations a) q (r) profile. The four horizontal lines - resonant q values. Triangle - q=1 position, circle - q=2 position; b) - radial locations of the bursts of the long distance toroidal correlations between the LFS and HFS

reflected layer radii from 6 to 24 cm. The reflection radial positions were found from the density profile obtained with 8 channel interferometer with λ=0.7 mm. Figures 5a and b present a safety factor q and experimentally observed long distance toroidal correlation maxima respectively plotted versus minor radius. The radial position of q=1 was found from SXR pin-hole chamber data as shown in Fig. 6 while q=2 radius was found directly from reflectometry measurements of m=2 island position [16] as shown in Fig. 7. Figure 7a shows the amplitude of the reflected wave phase oscillations caused by large scale MHD instability with m=2, n=1 versus minor radius. Figure 7b presents the calculated phase modulation of the reflected wave in 1D full wave approximation. An island-like density perturbation shown in Fig. 7c with the width 1.8 cm around q=2 position at r=20.6 cm was used in calculations. There are two maxima both in experimental data and in the model. It is typical result in the case of an island structure of density perturbation. Thus the position of q=2 can be found directly from reflectometry with high accuracy. Relative radial position of nearby toroidal correlation maxima with respect to q=2 position can be obtained with high precision with the help of the measurements of a slow variation of reflected wave phase. Unfortunately our investigations of m=1 oscillations with SXR pin-hole chamber show the presence of the kink perturbation but m=1 island was not observed. The absence of the island introduces the uncertainty in the determination of q=1 position. Figures 6 a, b show the radial dependencies of reflected wave phase jump in sawteeth crush (a) and m=1 amplitude (b). The amplitude of m=1 intensity fluctuations measured with SXR pin-hole chamber presented in Fig. 6c. And abelized and chord intensity jumps in sawteeth crash are shown in Fig. 6d and e respectively. It is clearly seen that the radial correspondence between reflectometry data and SXR one may be established very well from m=1 amplitude and jumps in sawteeth crashes radial dependences. It is shown by two vertical dashed lines in Fig.6. It is possible to relate m=1 position either with the inversion radius of abelized SXR intensity (r=9.6 cm in Fig.6d) or with m=1 appearance at r=8.5 cm in Fig.6b. The latter variant was chosen to plot q(r) dependence in Fig. 5a. A smooth curve passing through q=1, 2 and q(a)=3.54 was plotted. The radial positions,

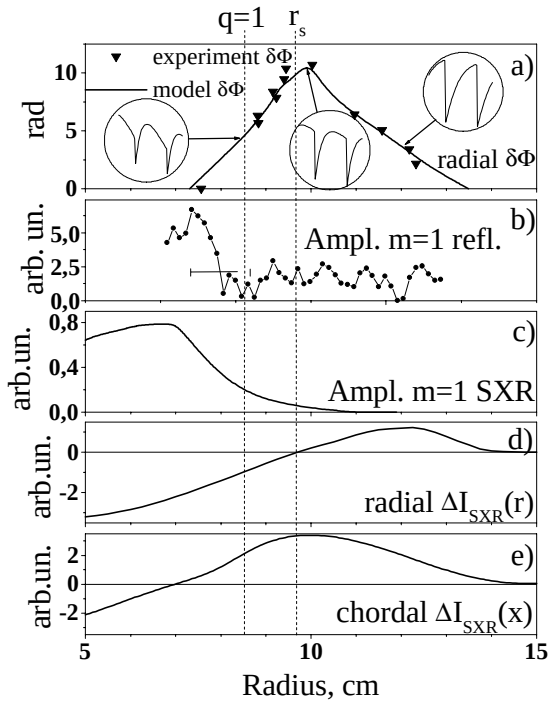

FIG. 6

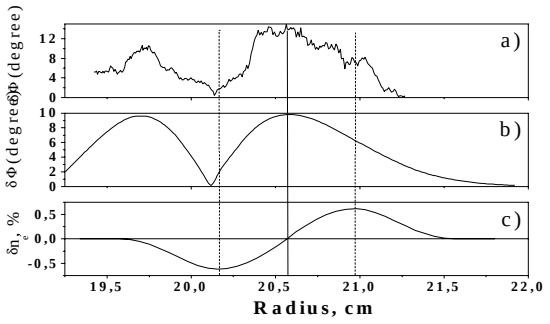

FIG. 7.

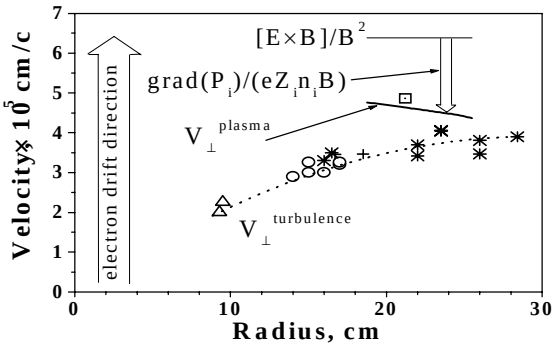

FIG. 8.

FIG. 6. Characteristics of sawtooth instability, measured with reflectometry and SXR pin-hole chamber. a)- The phase jump of reflected wave in sawteeth crash. Triangles - experiment; curve - simulation. The waveforms of the reflection phase are shown for three radii in circles. b) - m=1 amplitude from reflectometry; c) - m=1 amplitude from SXR; d) - abelized radial SXR intensity jump in sawteeth; e) - non-abelized SXR jump.

Fig. 7. Reflectometry measurements of the m=2 island radial position and width. a) - radial dependence of the experimental amplitude of the m=2 phase fluctuation; b) - the same as a) calculated with 1D full-wave code, c) - relative density perturbation, used in the model. Solid vertical line - q=2 radial position. Two vertical dashed lines show the island width.

Fig. 8. Comparison of the experimental turbulence rotation with calculated plasma one. Turbulence rotation: triangles - $n_e=1.05\times10^{19}m^{-3}$; circles - $n_e=1.3\times10^{19}m^{-3}$; crosses - $n_e=1.6\times10^{19}m^{-3}$; stars - $n_e=1.9\times10^{19}m^{-3}$. Top solid curve - $[E\times B]/B^2$ term; middle solid curve - resulting plasma rotation. Square - rotation of MHD oscillations with m=2.

amplitudes and the radial shape of the toroidal correlation maxima were taken from the experimental values of coherency between amplitude fluctuation of the waves reflected at LFS and HFS. The fluctuations were filtered in frequency range from 100 to 200 kHz. Four resonant values of 0.87, 1.16, 1.74 and 2.32 are shown by horizontal dashed lines in Fig. 5a, while q=1 and 2 are shown by the triangle and the circle respectively. One can see rather complicated pattern. Some maxima are near to resonant positions but still a number of them are at a distance $\Delta q\approx0.2$ from them. The deviation of correlation maxima from resonant position confirms oblique fluctuation propagation as was deduced from results presented in Fig. 4. The additional work to identify all the maxima are now in progress.

6. EVALUATION OF TURBULENCE ROTATION IN PLASMA FRAME

The direction and value of turbulence rotation in plasma frame are important parameters which may permit to identify the physical mechanisms of the turbulence. It can be found by comparison of fluctuation rotation with plasma one. A plasma rotation was estimated from a radial force balance

equation for ions using radial electric field measured with Heavy Ion Beam Probe diagnostic (HIBP) [17]. A perpendicular to magnetic field lines velocity was calculated according to the equation:

$$V\perp = [\mathbf{V}\times\mathbf{B}]/|B| = (-\nabla P_i/(eZ_i n_i) + E_r)/B$$

n_i, eZ_i and P_i are the ion density , charge and pressure, respectively; E_r is the radial electric field. A comparison of calculated plasma rotation perpendicular to the magnetic field with measured turbulence one is presented in Fig. 8. The plasma current was 140 kA, B_T =1.5 T and n_e from 1.2 to 2×10^{19} m^{-3}. The positive value of velocity corresponds to the rotation in electron diamagnetic drift direction. The lowest dashed curve is plotted as a spline of the experimental turbulence velocity obtained with different probing frequencies in discharges with different average densities. It is obvious that turbulence rotation doesn't depend on density. The upper horizontal curve shows E_r/B term calculated with the value of radial electric field 10^2 V cm^{-1}measured with HIBP [18]. The ion pressure term was calculated from 1D code [19] with neoclassical ion heat conductivity. The electron temperature was measured with SXR Pulse Height Analyzer technique and maximal ion temperature estimated from the intensity of neutron flux. The resulting plasma rotation is shown by the middle curve. The square is m=2 island rotation. It is seen that the turbulence velocity is less then that of the plasma in about 1×10^5 cm s^{-1}. It means that the turbulence rotates in ion diamagnetic drift direction in plasma frame and thus may have ion origin. Taken this velocity in plasma frame and the angle of propagation of 0.5^0 one can calculate the wave phase velocity along the magnetic field line V_{II} = 1.1×10^7 cm s^{-1}. The frequency of quasi-coherent turbulence is 135 kHz and rotation velocity $V_\perp=3.5\times10^5$ cm s^{-1} which give $\lambda_\perp$=2.6 cm, $k_\perp\times\rho_i$=0.3 and the longitudinal wavelength $\lambda_{II}\approx$3 m. The velocity along the magnetic field line is near to the ion thermal velocity $V_{Ti}=0.9\times10^7$ cm s^{-1} as should be for ITG mode. It is important to note that m=2 rotation also exceeds turbulence rotation and just coincides with plasma one. The same difference between the turbulence and m=2 rotation have been observed in a number of different discharges. The accuracy of these measurements enough high due to the fact that both measurements were obtained with the same reflectometry data. It may means that m=2 island is «frozen» into plasma and rotates together with it, but the turbulence rotates in ion diamagnetic direction with respect to plasma. It must be mentioned that the comparison of the turbulence and plasma rotation was carried out up to now only in one tokamak regime and involves rather complicated measurements of plasma potential and ion temperature gradient. It brings significant error in resulting plasma velocity. Taken this into account it is possible to conclude only that the turbulence either rotates in ion diamagnetic drift direction or at least is at rest in a plasma frame. But the additional facts of oblique wave propagation and difference between turbulence and MHD rotation enable us to conclude that turbulence rotates with respect to the plasma in ion diamagnetic drift direction.

7. CONCLUSIONS

The experimental data showed the presence of two turbulence types in the frequency range of the drift waves in ohmic tokamak discharges. Both turbulences propagate at an angle of about 0.5^0 with respect to a direction perpendicular to the total magnetic field line as is expected for the drift waves. They have longitudinal correlation lengths more then 10 m and rotates in ion diamagnetic drift direction in plasma frame. The first one, referred to as «quasi-coherent» fluctuations [7], is highly asymmetrical poloidally and has typically $\lambda_\perp$=2÷3 cm and $k_\perp\times\rho_i$=0.5÷0.3. The second is poloidally symmetrical and has $\lambda_\perp$=1÷1.7 cm and $k_\perp\times\rho_i$=1÷0.5. All experimental observations are consistent with the Toroidal and Slab ITG physical mechanism of turbulence.

ACKNOWLEDGMENTS

The authors is grateful to the experimental and operational T-10 teams, who run T-10 and provide the experimental data about discharge parameters. Special thanks to Dr. Merezhkin for the neoclassical calculations and Drs. Sushkov and Kirneva for SXR measurements. This work has been carried out under financial support of the Russian Foundation of Basic Research. Grant # 96-02-18807.

REFERENCES

[1] S.F. Paul, N. Bretz, R.D. Durst, et al, Phys. Fluids B 4 (1992) 2922.
[2] L.L. Lao, K.H. Burrel, T.S. Casper, et al, Phys. Plasmas (1996) 1951.
[3] Rudakov L.I., Sagdeev R.Z., Nuclear Fusion Supplement, 1962, 2, 481 (1962).
[4] B.B. Kadomtsev, O.P. Pogutse, in Reviews of Plasma Physics (M.Leontovich, Consultants Bureau, New York, 1970), Vol. 5, p. 249.
[5] R.D. Durst, R. J. Fonk, J.S. Kim et al, Phys. Rew. Letters (1993) 3135.
[6] Vershkov V.A., et al, 15th IAEA Conference in Plasma Phys. and Contr. Fus. Res., Seville, 1994, Vol. 2, IAEA, Vienna (1995) 65.
[7] Vershkov V.A., et al, 22 EPS Conference on Contr. Fus. And Plasma Phys. Bournemouth, 1995, Vol. 19 C, Part 4, p. 5
[8] Vershkov V.A., et al, (Proceedings of 12th International PSI Conference, Saint Raphael, France, 1996), Journal of Nuclear Matter. V 241-243 (1997) 873.
[9] Vershkov V.A. et al, 16th IAEA Conference in Plasma Phys. and Contr. Fus. Res., Montreal, 1996, Vol. 1, IAEA, Vienna (1997) 519.
[10] Vershkov V.A., et al, 24 EPS Conference on Contr. Fus. And Plasma Phys. Berchtesgarden, 1997, Vol. 21A, Part 2, p. 665.
[11] Fussmann G., et al, 12th IAEA Conference in Plasma Phys. and Contr. Fus. Res., Nice, 1988, Vol. 1, IAEA, Vienna (1989) 145.
[12] Horton W. Jr., Choi Duk-In, Tang W.M., Physics of Fluids, 24, 1077, (1981).
[13] Vershkov V.A, et al, 21th EPS Conference in Plasma Phys. and Contr. Fus. Res., Montpellier, France, 1985, Vol. 18 B, part 2, p 886.
[14] V.V. Alikaev et al, Plasma Phys. And Contr. Fus., V 30, (1988) 381.
[15] M.Frances et al, 22 EPS Conference on Contr. Fus. And Plasma Phys. Bournemouth, 1995, Vol. 19C, Part IV, p. 429.
[16] Soldatov S.V., et al, 24 EPS Conference on Contr. Fus. And Plasma Phys. Berchtesgarden, 1997, Vol. 21A, Part 2, p. 673.
[17] V.I. Bugaria, V.I. Gorshkov, S.A. Grashin, et al, Nuclear Fusion V 25 (1985) 1707.
[18] Melnikov A.V.,et al, 23 EPS Conference on Contr. Fus. And Plasma Phys. Kiev, Ukrainie, 1996, Vol. 20C, Part 1, p. 436.
[19] Merezhkin V. G., et al, Russian Fizika Plasmy, **14**, (1988)131.